Low-temperature MOCVD deposition of Bi_2Te_3 thin films using $Et_2BiTeEt$ as Single Source Precursor.

Georg Bendt[1], Sanae Gassa[1], Felix Rieger[2], Christian Jooss[2] and Stephan Schulz[1]*

[1]Institute of Inorganic Chemistry and Center for Nanointegration Duisburg-Essen (CENIDE), University of Duisburg-Essen, Universitätsstr. 5-7, D-45117 Essen, Germany. Fax: 49 0201 1833830; Tel: 49 0201 1834635; E-mail: stephan.schulz@uni-due.de

[2]Institute for Materials Physics, University of Göttingen, Friedrich-Hund-Platz 1, D-37077 Göttingen, Germany.

Abstract

$Et_2BiTeEt$ was used as *single source precursor* for the deposition of Bi_2Te_3 thin films on Si(100) substrates by metal organic chemical vapor deposition (MOCVD) at very low substrate temperatures. Stoichiometric and crystalline Bi_2Te_3 films were grown at 230 °C, which is approximately 100 °C lower compared to conventional MOCVD processes using one metal organic precursors for each element. The Bi_2Te_3 films were characterized using scanning electron microscopy, high-resolution transmission electron microscopy and X-ray diffraction. The elemental composition of the films, which was determined by energy-dispersive X-ray spectroscopy and X-ray photoelectron spectroscopy, was found to be strongly dependent of the substrate temperature.

Keywords. A3. Metalorganic chemical vapor deposition, B1. Bismuth compounds, B1. Tellurides, B1. Nanomaterials, B2. Semiconducting materials

Introduction

Thermoelectric materials allow the direct conversion of heat into electrical power without the use of mechanic transmission. Despite the inefficiency of thermoelectric materials for large scale energy generation[1], these materials are ideal for harvesting energy for sensors and other small devices. The thermoelectric efficiency of a material is given by the dimensionless figure of merit $ZT = (S^2\sigma/\kappa)T$ (S = Seebeck coefficient, σ = specific electrical conductivity, κ = thermal conductivity = sum of electronic κ_{el} and lattice κ_{la} contributions, T = absolute temperature [K])[2]. Bi_2Te_3 combines a high Seebeck coefficient and high electrical conductivity with a glass-like low thermal conductivity, resulting in a superior thermoelectric performance near room temperature. However, the synthesis of high-quality Bi_2Te_3 materials such as nanoparticles and thin films is very challenging, especially due to the high tendency of Bi_2Te_3 to form antisite defects. In particular, the incorporation of excess bismuth into the crystal lattice and subsequent formation of sandwich-like structures of the general form $(Bi_2)_n(Bi_2Te_3)_m$ are generally observed for tetradymite-type materials[3].

Metal organic chemical vapor deposition (MOCVD) is a widely used industrial process for the deposition of Bi_2Te_3 films, in which metal organic compounds such as trialkyl bismuth (R_3Bi) and dialkyl tellurium (R_2Te) are typical precursors. For example, Giani et al. reported on the growth of Bi_2Te_3 films using trimethyl bismuth (Me_3Bi, TMBi) and diethyl tellurium (Et_2Te, DETe) at 450 °C on pyrex and silicon substrates[4], while You et al. successfully grew Bi_2Te_3 thin films using TMBi and diisopropyl tellurium (*i*-Pr_2Te, DIPTe) at 400 °C on GaAs(001) substrates[5]. Alternative tellurium precursors such as diethyl ditelluride (Et_2Te_2, DEDTe) and triethyl bismuth (Et_3Bi, TEBi) were also used for the deposition of highly *c*-oriented Bi_2Te_3 on Al_2O_3(0001) at 400 °C[6]. To the best of our knowledge, thin film deposition at lower substrate temperatures (300 °C) was only achieved by Kang et al. using a combination of TEBi and di-tertiarybutyl tellurium (*t*-Bu_2Te, DTbTe) on SiO_2 substrates[7]. For these specific types of tetradymite materials, lower substrate temperatures have several advantages including energy saving and lower processing costs, but most importantly, the formation of antisite defects - in this case, the replacement of Te atoms by Bi atoms - can be reduced. The formation of antisite defects strongly correlates with the synthetic conditions; its formation is favored at high temperature and low pressure conditions due to the high vapor pressure of elemental Te. Consequently, low deposition temperatures are advantageous for the synthesis of highly-stoichiometric Bi_2Te_3 materials.

In addition to simple binary tetradymite-type films, the deposition of multilayer structures has been previously investigated. Venkatasubramanian et al. reported on record-high *ZT* values of up to 2.4 at 300 K for p-type Bi_2Te_3/Sb_2Te_3 superlattice devices, which was ascribed to an effective control of the transport of phonons and electrons in the superlattices[8]. However, such high *ZT* values have never been reproduced by other groups, thus the applicability of this concept was questioned[9]. In particular the low thermal stability of Bi_2Te_3/Sb_2Te_3 superlattices was found to hamper their potential use in technical applications[10-12].

Single source precursors (SSPs) have been shown to be very promising candidates for low-temperature deposition processes. Chivers et al. reported on the deposition of Sb_2Te_3 nanoplates by *aerosol assisted chemical vapor deposition* (AACVD) using $[Sb\{(TeP^iPr_2)_2N\}_3]$[16], while alkylchalcogenostibines $Ph_2SbTeEt$ and $MeSb(TeBu)_2$ were used by Kim et al. and Reid et al. as SSP for the solution-based formation of Sb_2Te_3-nanoplates and the chemical vapor deposition of Sb_2Te_3 thin films, respectively[17-19]. We recently demonstrated that the thermal decomposition of the SSP $(Et_2Sb)_2Te$ in solution-based[13,14] and gas-phase-based processes[15] allowed the generation of highly stoichiometric, crystalline Sb_2Te_3 nanoparticles and thin films at rather low temperatures (180-200 °C). These nanomaterials exhibited very high Seebeck coefficients, indicating low concentrations of antisite defects.

So far, there has been no report on SSPs being successfully used in the deposition of Bi_2Te_3 thin films, or in the solution-based synthesis of Bi_2Te_3 nanoparticles. Despite the limited number of stable bismuth-tellurium containing molecules[20], these compounds remain highly sensitive to air, moisture, light, and temperature. Attempts to investigate $(Et_2Bi)_2Te$ and $Et_2BiTeEt$ as potential SSPs for the wet chemical synthesis of Bi_2Te_3 in organic solvents[21] were not fruitful. The thermal decomposition of both precursors only resulted in the formation of Bi-rich phases (i.e. Bi_4Te_3 and Bi_2Te), most likely due to the weak Bi-C bond.

To the best of our knowledge, there has only been a single report on the successful use of a Bi-Te containing SSP by MOCVD methods; Reid et al. deposited high-quality Bi_2Te_3 thin films using the bismuth telluroether complex $[BiCl_3(TeBu_2)_3]$[22]. Unfortunately, high substrate temperatures are required to achieve acceptable growth rates due to the strong Bi-Cl bond, which is a severe drawback of this precursor. In addition, the use of chloride-containing precursors should generally be avoided due to their corrosive nature.

Experimental

$Et_2BiTeEt$[23-25] was freshly prepared for each MOCVD study by mixing equimolar amounts of Et_2Te_2 and Et_4Bi_2 under argon atmosphere inside a glovebox. $Et_2BiTeEt$ was obtained as a red liquid via an exchange reaction (Scheme 1), typically occurring between dipnictogenes R_4E_2 (R = alkyl, aryl; E = Sb, Bi) and dichalcogenanes R_2X_2 (R = alkyl, aryl; X = S, Se, Te)[23,24].

Scheme 1. Synthesis of $Et_2BiTeEt$.

$$Et_2Bi{-}BiEt_2 + EtTe{-}TeEt \longrightarrow 2\ Et_2Bi{-}TeEt$$

The thermal properties of $Et_2BiTeEt$ make this molecule very promising for MOCVD studies. According to our differential scanning calorimetry (DSC) study[21], the thermal decomposition of $Et_2BiTeEt$ starts at 85 °C with the formation of Et_3Bi and Et_2Te, which were found to decompose at higher temperatures (225 °C and 270 °C, respectively). Thermal decomposition of a solution of $Et_2BiTeEt$ in diisopropylbenzene at 100 °C only yielded bismuth-rich Bi_2Te phase rather than the Bi_2Te_3 phase. The decomposition is most likely initiated with the homolytic cleavage of the Bi-Te bond and the subsequent formation of $Et_2Bi\cdot$ and $EtTe\cdot$ radical species. These radicals react to give Et_3Bi ($3Et_2Bi\cdot \rightarrow 2Et_3Bi + Bi$) and Et_2Te ($2EtTe\cdot \rightarrow Et_2Te + Te$), along with elemental Bi and Te, which ultimately form binary bismuth telluride phases.

MOCVD Deposition. MOCVD studies were performed in a hot-wall MOCVD reactor. Bi_2Te_3 films were deposited on Si(100) substrates at a working pressure of 10 mbar. Si(100) substrates were degreased with acetone, treated with hydrofluoric acid and heated to 500 °C at 10^{-3} mbar for 1 hour in the reactor. Argon was used as carrier gas (40 sccm). The temperature and pressure of the precursor's glass bubbler were kept constant at 25 °C and atmospheric pressure, respectively. Upon completion of the film deposition (growth time = 15 minutes), the system was cooled to ambient temperature within 30 minutes.

X-ray photoelectron spectroscopy. XPS studies were performed using a Versaprobe IITM (Ulvac-Phi) with monochromatic Al K_α light at 1486.6 eV photon energy. The emission angle between analyzer and the sample was 45°. The Cu 2p signal at 932.67 eV binding energy, which was obtained with a sputter cleaned Cu foil, was used as the binding energy reference. The foil and powder were adhered onto insulating double-sided tape, while charging effects were compensated with a dual-beam neutralizing approach using electrons and slow-moving argon ions.

Electron microscopy. Morphology and elemental composition of the films were analyzed by scanning electron microscopy (SEM) using a Jeol JSM 6510 microscope equipped with a Bruker Quantax 400 EDX spectrometer. The relative error for the EDX determination was calculated using

the Esprit 4.0 software from Bruker.

HRTEM studies were conducted using a CS image corrected FEI TITAN with a lateral resolution limit of 0.08 nm at 300 kV. TEM lamellas were prepared in an FEI Nova Nanolab600 FIB. A 30 kV accelerator voltage was used to cut the lamellas in the first thinning steps, while 5 kV were applied for the last thinning step in order to reduce knock-on damage by the Ga ions.

X-ray powder diffraction. Grazing incidence X-ray powder diffraction (GIXRD) patterns were obtained at ambient temperature (25 ± 2°C) using a Panalytical Empyrean diffractometer with CuK_{α} radiation (λ = 1.5418 Å, 40 kV, 40 mA) and a fixed angle of incidence of 1°. The films were investigated in the range of 5–90° 2Θ with a step size of 0.05° 2Θ.

Results and Discussion

Film deposition studies were performed at different substrate temperatures of 215 °C, 230 °C and 245 °C. The formation of dense films required a minimum substrate temperature of 230 °C, while lower substrate temperature resulted in the growth of isolated Bi_2Te_3 platelets (Fig. 1). A dense film was also obtained at 245 °C, but EDX studies revealed that this film does not show the expected 2:3 molar ratio (Bi:Te) but rather a 4:3 molar ratio, pointing to the formation of Bi-rich Bi_4Te_3.

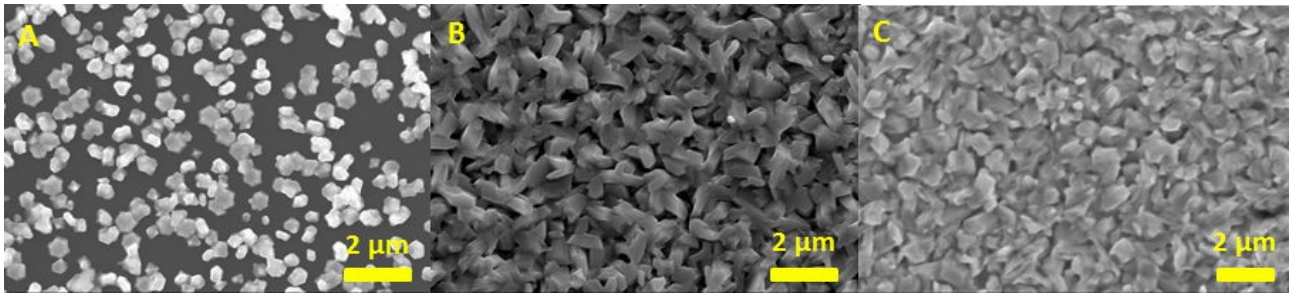

Figure 1. SEM picture of isolated Bi_2Te_3 hexagons grown at 215 °C (**A**) and dense bismuth telluride films grown at 230 °C (**B**) and 245 °C (**C**).

The morphology of the silver-grey Bi_2Te_3 film deposited at 230 °C was investigated in detail by scanning electron microscopy (SEM). The images reveal that the dense film consists of intergrown 250 nm thick grains (Fig. 2). A cross section photograph of the film shown in Fig. 2C clearly indicates that the Bi_2Te_3 film is built with the grains laid or standing tilted on the surface of the substrate.

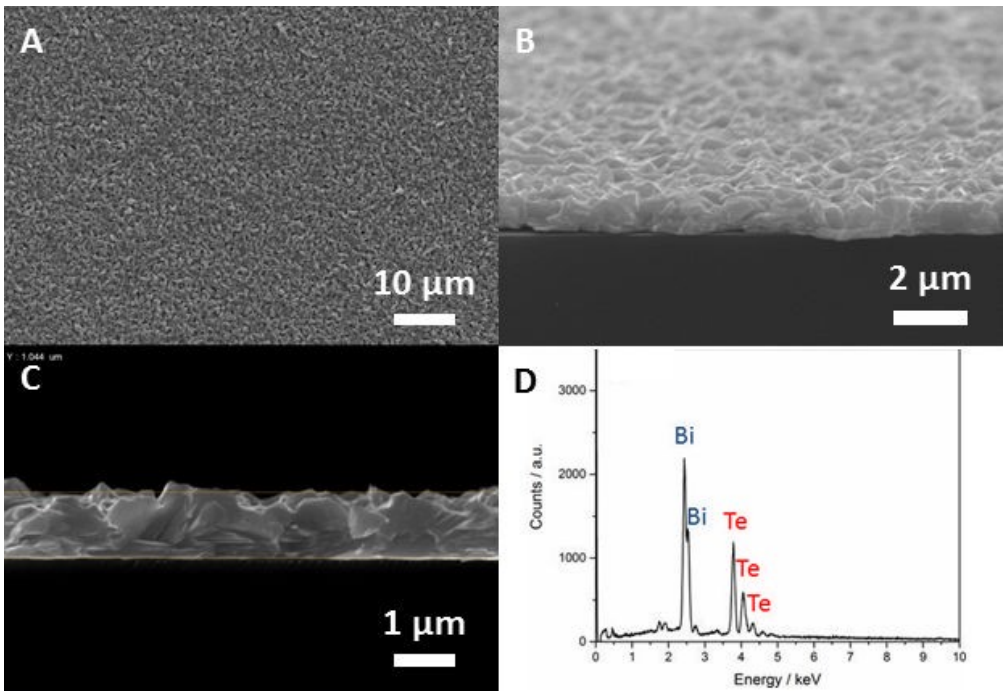

Figure 2. SEM images at different magnifications (**A**, **B**) and cross section photographs (**C**) of a Bi_2Te_3 film grown at 230 °C on a Si(100) substrate; EDX spectrum (**D**) of the Bi_2Te_3 film.

Energy-dispersive X-ray (EDX) spectra of the films show the characteristic peaks for bismuth at around 2.5 keV, and for tellurium at around 4.0 keV (Fig. 2D). In addition, small peaks for carbon at 0.3 keV and oxygen at 0.5 keV were also observed. Quantitative elemental analysis reveals that the Bi:Te ratio of the films grown on Si(100) substrates strongly depends on the substrate temperature. Values close to the theoretical value for Bi_2Te_3 (40:60) were obtained for films grown at 215 °C and 230 °C, whereas growth at 245 °C yielded a Bi-rich film (Table 1).

Table 1. Elemental composition of bismuth telluride films grown at different substrate temperatures on Si(100) substrate as determined by EDX, and growth rates for the deposition of dense films at 230 °C and 245 °C.

	215 °C	**230 °C**	**245 °C**
Bi	39.9±1.0[a]	40.4±1.3	48.4±0.9
Te	60.1±0.9	59.6±1.1	51.6±0.8
Growth rate µm·h^{-1}	---	4.0	4.8

[a] The EDX error was calculated using the software Esprit 4.0 from Bruker.

The crystallinity of the films was investigated by X-ray diffraction (XRD). The patterns were measured in grazing incidence geometry (GIXRD). All observed Bragg reflections can be indexed on the basis of rhombohedral Bi_2Te_3 (PDF card 15-0863) and Bi_4Te_3 (PDF card 33-216). Peaks indicating

the formation of other bismuth telluride phases, oxidation products such as Bi_2O_3, Sb_2O_3, TeO_2 or elemental Te were not detected.

The surface sensitive GIXRD pattern allows a clear phase identification of the deposited material films (Fig. 3). The GIXRD patterns obtained from the films deposited at 215 °C and 230 °C can both be indexed on the basis of phase pure Bi_2Te_3, whereas the film deposited at 245 °C shows the presence of Bi-rich Bi_4Te_3 as secondary phase, confirming the EDX results. The differentiation between the two bismuth telluride phases is challenging since the structural differences are very small, and therefore resulting in similar XRD patterns. In this case, the different positions of the 006 reflections around 17.6 ° were used.

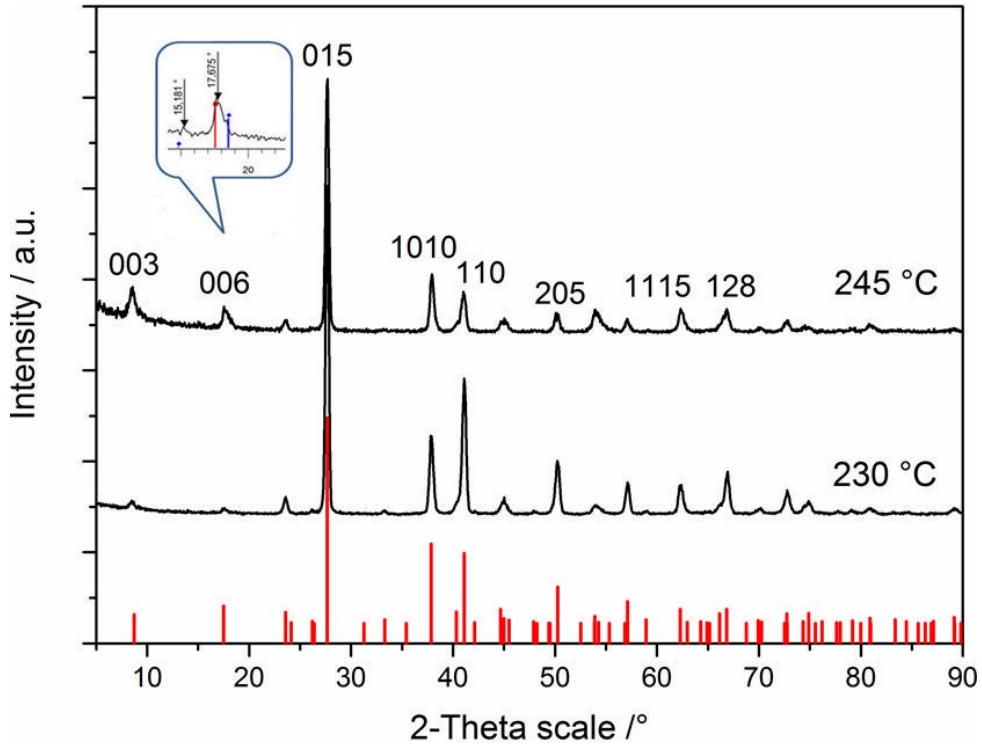

Figure 3. GIXRD pattern of Bi_2Te_3 films deposited at 230 °C and 245 °C on Si(100) substrates; most intense peaks are labelled and correspond to the expected reflections of Bi_2Te_3 (PDF card 15-0863).

In order to gain more information on the film texture and the orientation of the crystallites on the substrate surface, pole figures were measured for two reflections in the Bi_2Te_3 film grown at 230 °C on Si(100). The (105) pole figure displayed in 2D and 3D representations (Fig. 4) was measured at $2\Theta = 27.64°$. The results showed a strong intensity in the center of the figure at $\psi = 90°$, and a narrow ring structure at $\psi = 45°$. The pole figure suggests that the majority of the Bi_2Te_3 grains are standing tilted on the substrate surface, as observed in the SEM cross section image (Fig. 2), whereas a minor part of the grains lies flat on the substrate surface.

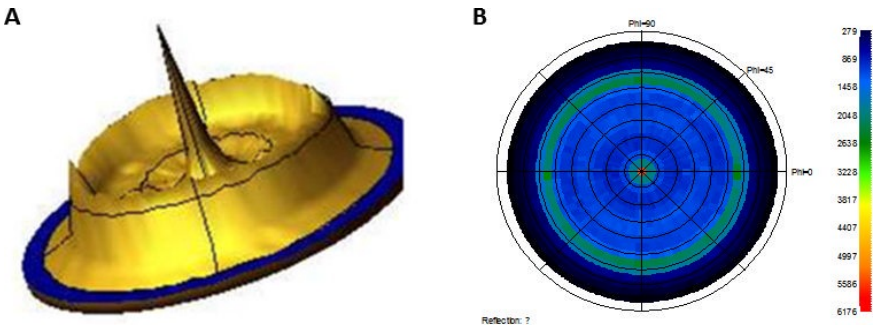

Figure 4. Pole figure for the (105) reflection of the Bi_2Te_3 film deposited at 230 °C on a Si(100) substrate in 3-dimensional (**A**) and 2-dimensional (**B**) representation.

X-Ray photoelectron spectroscopy (XPS) is a surface sensitive method for the determination of the chemical environment of an element. XPS measurements of the Bi_2Te_3 film grown at 230°C on Si(100) revealed the expected peaks for Bi 4f7/2 and Bi 4f5/2 at 157.5 and 162.8 eV, as well as the expected peaks for Te 3d3/2 and Te 3d5/2 at 582.9 and 572.5 eV (Fig. 5), respectively. These values are in good agreement with the reported binding energies of Bi_2Te_3[26-29]. In addition, a second set of peaks at higher binding energy is visible for every element, comparable to the binding energies in Bi_2O_3 and TeO_2. Since only one O 1s peak at 530.3 eV was observed, the film surface is most likely covered with a thin layer of $Bi_2Te_{3-x}O_x$. Surface oxidation was expected since the film was handled and transferred under ambient conditions, leading to the post-growth oxidation of the material. This was proven by an elemental depth profile analysis, showing a strong decrease of the oxidized species after a short sputtering period. After a sputtering time of 3 min, with an acceleration voltage of 3 kV corresponding to an abrasion of about 10 nm equivalent to 10 quintuple layers, the intensities of the peaks corresponding to oxygen or carbon are below the detection limit. The surface oxidation of Bi_2Te_3 and other tetradymite type materials has been previously reported[30,31].

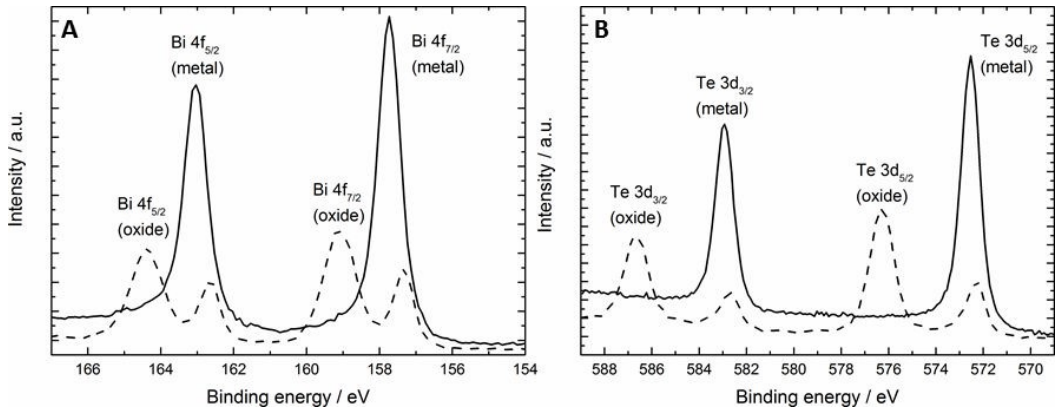

Figure 5. Bi 4f (A) and Te 3d (B) core level XPS spectra of Bi_2Te_3 thin films before (dashed line) and after sputtering (solid line).

A transmission electron microscopy (TEM) lamella image was taken by using the focused ion beam technique to inspect the film's microstructure and film-substrate interface in cross-section for the Bi_2Te_3 film grown at 230 °C.

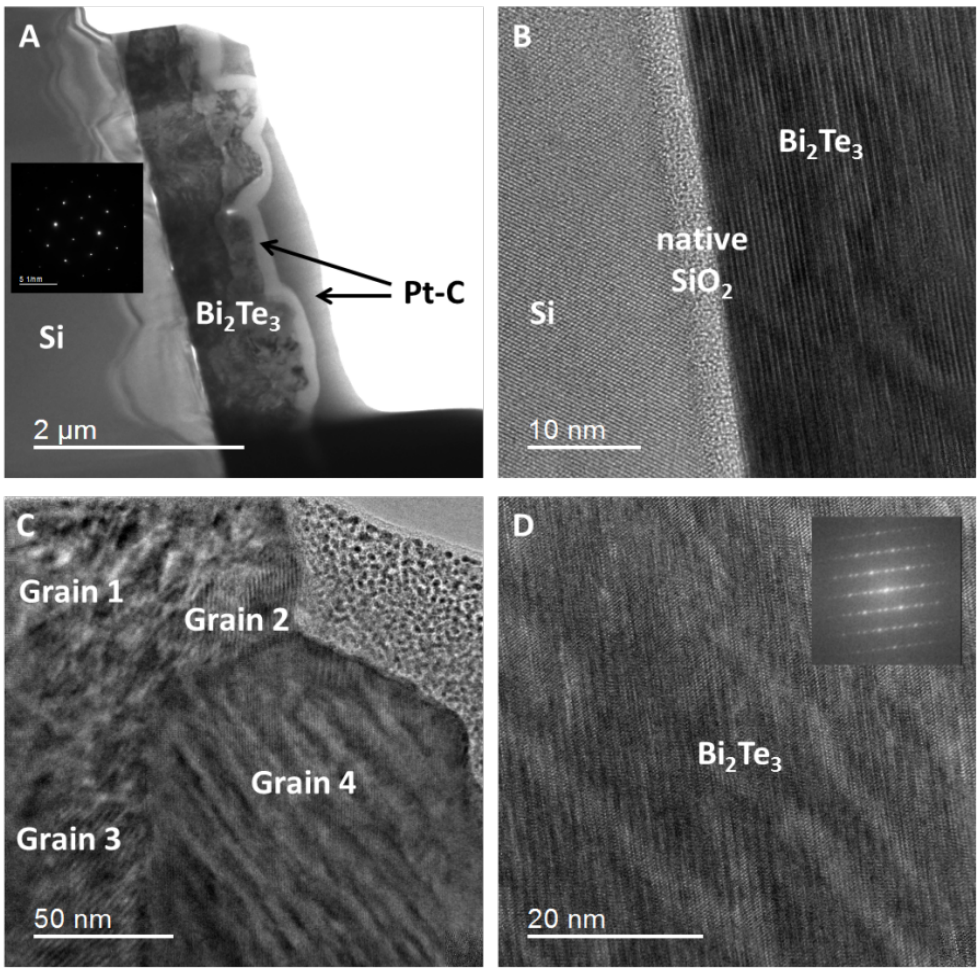

Figure 6. TEM overview image of a FIB cut cross-section lamella (**A**), HRTEM image of the film-substrate interface (**B**), HRTEM image showing multiple grains close to the film surface (**C**) and HRTEM image of a region inside a c-oriented Bi_2Te_3 grain (**D**).

An overview of a bright field image of the lamella (Fig. 6A), defocused by 5 µm for better visibility of grain boundaries, displays the Bi_2Te_3 film with a non-uniform thickness of around 0.8 to 1.0 µm. In addition, both platinum layers, which were deposited during the FIB process to protect the film, are visible. The selected area electron diffraction (SAED) pattern showing the substrate orientation is presented as inset in Fig. 6A. At a higher magnification, the image reveals a sharp interface between the native SiO_2 layer and the Bi_2Te_3 film (Fig. 6B). The lattice fringes with a spacing of 1 nm parallel to the interface are consistent with the initial c-oriented growth of Bi_2Te_3 on the Si (100) substrate, which can be observed at the lower part of the film. Fig. 6C shows different grains in the upper part of the film. A HRTEM image of a c-oriented grain is shown in Fig. 6D. The inset displays

the corresponding diffraction pattern, generated by a Fast Fourier Transformation. Furthermore, Figs. 6C and 6D show diagonal stripe patterns that arise from a high density of local stacking faults with a lateral extension of approximately 10 nm. Partial dislocations can terminate such stacking faults.

The low substrate temperatures (215 to 245 °C) in our MOCVD experiments are expected to stimulate the growth of polycrystalline films due to the reduced mobility of the adatoms on the substrate surface during film growth, which is a pre-requisite for the formation of smooth c-oriented films. Comparable findings were observed in the low-temperature MOCVD growth of Sb_2Te_3 films using $(Et_2Sb)_2Te$ as SSP[15] and was reported for the ALD growth of Sb_2Te_3 and Bi_2Te_3 films[32-34], which were also found to be strongly temperature-dependent. The film growth occurred via a Volmer–Weber island growth mechanism and initially formed Sb_2Te_3 and Bi_2Te_3 grains, which then coalesced to a smooth film with increasing number of cycles, and finally resulted in the formation of three-dimensional polycrystalline Sb_2Te_3 and Bi_2Te_3 films, respectively. However, we observed the formation of c-oriented platelets in the early stage of the growth process, especially at low temperature (see also fig. 2), which then leads to the formation of a polycrystalline film. One possible reason for this phenomenon could be an influence of the substrate material. It is well known that the morphology of MOCVD- and ALD-grown Sb_2Te_3 and Bi_2Te_3 films is strongly influenced by the substrate material. For instance, flat c-oriented films were formed on OH-terminated oxide interfaces of Si or SiO_2 substrates[7,32,35,36] as well as Al_2O_3 substrates[6]. These studies clearly demonstrate that the early state of the film growth shows a strong preference for the growth of c-oriented platelets, but is always accompanied by the minor formation of platelets, which adopt other orientations. We believe that the OH-termination of the native oxide surface of the Si(100) substrates, which were used without further chemical or thermal pretreatment, enhances the growth of flat c-oriented platelets in the early stage of the film growth, which is also visible in the SEM images (Fig. 2). The preferential c-oriented growth of Bi_2Te_3 on SiO_2 at low temperatures is phenomenologically described in Ref. 7. Once the initially formed platelets coalesce into a dense film, the relative growth rates on diverse plane orientations enhance the growth of platelets of different orientations, which results in the formation of rough films with a significant number of grains.

The formation of crystalline, phase-pure Bi_2Te_3 films at low substrate temperature is remarkable. A very recent study on the growth of bismuth telluride thin films by a classical *two-precursors* MOCVD process using TMBi, DETe and H_2 revealed that the quality of the resulting films strongly

depends on the substrate temperature and the precursor stoichiometry[37]. The lowest substrate temperature, at which Bi_2Te_3 film growth was observed, was 330 °C. However, phase-pure, crystalline Bi_2Te_3 films were obtained at this substrate temperature only in the presence of a very large excess of DETe (Te:Bi ratio > 30), while at higher temperatures, the excess of DETe can be reduced (420 °C: Te:Bi 10; 463 °C: Te:Bi 5)[37]. In our case, the use of the SSP $Et_2BiTeEt$ does not require any excess of Te, especially since the precursor decomposes in a stoichiometric reaction on the surface of the substrate, and therefore allows the growth of Bi_2Te_3 films at significantly lower temperatures (230 °C). Although surface-controlled reactions are often known to require lower temperatures in comparison to gas phase decomposition reactions, this is not always case. For instance, *t*-Bu_3Al decomposes in the gas phase at 250 °C, whereas 277 °C is required on the surface[38]. Gas phase reactions are expected to play a major role at high process temperatures, and more importantly, at high process pressures since they are initiated by the collisions between molecules[39]. Therefore, low process temperatures (200 - 250 °C) in combination with reduced pressure conditions (10 mbar) are expected to reduce unwanted gas phase reactions, which could potentially lead to the synthesis of Bi_2Te_3 nanoparticle in the gas phase. This whole process could be transformed into a surface-decomposition controlled MOCVD process. In addition, the gas phase decomposition of $Et_2BiTeEt$ is likely to occur with the breakage of the Bi-Te bond as it's the weakest chemical bond in this compound, thus leading to the formation of $Et_2Bi\cdot$ and $EtTe\cdot$ radical species. $EtTe\cdot$ radicals may either recombine to form Et_2Te_2, which is thermally stable as observed with Me_2Te_2[40], or further react to give Et_2Te and Te vapor. Et_2Te is also thermally stable and starts to decompose at 272 °C according to previous DSC studies[21]. In this case, most of the tellurium would be transferred out of the reactor instead of being used in the film growth, and therefore leading to the formation of Bi-rich films. Moreover, the *dual source* MOCVD growth of Bi_2Te_3 films using Et_2Te and Et_3Bi only results in Bi_2Te_3 film growth at temperatures of at least 350 °C,[41] which is roughly 120 °C higher than our SSP approach $Et_2BiTeEt$. These findings are in accordance with previous dual source MOCVD growth studies[4-6]. To further exclude the possibility of a gas phase decomposition process, we performed an experiment in which the precursor was passed through a glass tube that was heated up to 215 - 245 °C and the substrate was placed in the cold zone at the end of the oven. We did not observe the formation of a Bi_2Te_3 film, which would have been expected in case Bi and Te vapor are formed by the gas phase decomposition of the precursor as described above.

The growth of stoichiometric Bi_2Te_3 films at 230 °C strongly supports the surface-controlled decomposition process. In particular, $Et_2BiTeEt$ does not decompose into $Et_2Bi\cdot$ and $EtTe\cdot$ radical spe-

cies in the gas phase, but instead absorbs as intact molecules on the surface of the substrate, thus behaving as a "true" *single source precursor*. The growth mechanism is likely initiated by the homolytic breakage of the Bi-Te bond, which then triggers the multi-step decomposition of $Et_2BiTeEt$ on the surface of the substrate. The resulting $Et_2Bi\cdot$ and $EtTe\cdot$ radicals undergo disproportionation reactions with subsequent formation of Et_3Bi and Et_2Te, as well as elemental bismuth and tellurium:

$$6Et_2BiTeEt \rightarrow 6Et_2Bi\cdot + 6EtTe\cdot$$

$$6Et_2Bi\cdot \rightarrow 4Et_3Bi + 2Bi$$

$$6EtTe\cdot \rightarrow 3Et_2Te + 3Te$$

These decomposition reactions yield Bi and Te in the correct 2:3 stoichiometric ratio, hence results the growth of stoichiometric Bi_2Te_3 films. At higher substrate temperatures (245 °C), Et_3Bi was shown to further decompose (at least partially) and give Bi-rich Bi_4Te_3 films. Control of the substrate temperature therefore is crucial for the deposition of phase-pure Bi_2Te_3 films, as was also observed in dual source processes[37]. In this case, the SSP $Et_2BiTeEt$ allows for the use of lower substrate temperatures without any excess of Te precursor. A similar behavior was observed with $(Et_2Sb)_2Te$ as a SSP for the MOCVD growth of Sb_2Te_3 thin films[15]. Despite the Sb:Te ratio of 2:1, its thermal decomposition leads to highly stoichiometric Sb_2Te_3 both in solution and in gas phase processes. This is because the formation of volatile Et_3Sb from the decomposition of $(Et_2Sb)_2Te$ easily transfers excess antimony out of the reactor.

Conclusion.

The potential application of $Et_2BiTeEt$ as a SSP for the MOCVD growth of Bi_2Te_3 films on Si(100) substrates was demonstrated. The single source approach allows the growth of Bi_2Te_3 films at very low substrate temperatures of 230 °C, whereas conventional “dual source” precursors typically require significantly higher substrate temperatures at around 400 °C, as well as large excess of the Te precursor. The low deposition temperature of 230 °C, which is significantly lower than the decomposition temperature of the expected decomposition product Et_2Te (270 °C according DSC) and lower than reported MOCVD processes using Et_3Bi and Et_2Te, indicates that $Et_2BiTeEt$ is stable in the gas phase under the specified process conditions and adsorbs as intact molecules on the substrate surface, hence serving as *single source precursor* for the Bi_2Te_3 film growth. EDX and XRD studies revealed the formation of highly stoichiometric and phase pure Bi_2Te_3 films at 215 and 230 °C, while higher substrate temperatures (245 °C) yielded Bi-rich materials with Bi_4Te_3 as additional phase. XPS studies proved the existence of a thin oxide layer on the film surface due to

post-deposition surface oxidation reactions. To the best of our knowledge, this study represents the first report on the successful growth of crystalline Bi_2Te_3 thin films at low substrate temperatures using a metal organic SSP. We are currently investigating the low-temperature film growth on different substrates as well as with different SSPs, in which the Bi:Te ratio is systematically varied in order to reveal the influence of both parameters on the morphology (and composition) of the resulting Bi_2Te_3 films.

Acknowledgment. F.R. and C.J are grateful to V. Roddatis for support of HRTEM characterization. Financial support by the Deutsche Forschungsgemeinschaft DFG (S. Schulz, project SCHU 1069/20-1; C. Jooss, project JO 348/12-1) is acknowledged.

References

[1] C. B. Vining, *Nat. Mater.* **2009**, *8*, 83.

[2] D. M.Rowe, CRC Handbook of Thermoelectrics, CRC Press, Boca Raton, **1995**.

[3] J. W. G. Bos, H. W. Zandbergen, M. H. Lee, N. P. Ong, R. J. Cava, *Phys. Rev. B* **2007**, *75*, 195203.

[4] A. Giani, A. Boulouz, F. Pascal-Delannoy, A. Foucaran, E. Charles, A. Boyer, *Mater. Sci. Engin. B* **1999**, *64*, 19.

[5] H. You, S. H. Baek, K.-C. Kim, O. J. Kwon, J.-S. Kim, C. Park, *J. Cryst. Growth* **2012**, *346*, 17.

[6] S. Schulz, G. Bendt, J. Sonntag, A. Lorke, U. Hagemann, W. Assenmacher, *Semicond. Sci. Technol.* **2015**, *30*, 085021.

[7] S.-W. Kang, K.-M. Jeon, J.-S. Shin, J.-R. Chun, Y.-H. Kim, S. J. Lee, J.-Y. Yun, *Chem. Vap. Deposit.* **2013** *19*, 61.

[8] R. Venkatasubramanian, E. Siivola, T. Colpitts, B. O'Quinn, *Nature* **2001**, *413*, 597.

[9] For a recent review article see: T. Dankwort, A.-L. Hansen, M. Winkler, U. Schürmann, J. D. König, D. C. Johnson, N. F. Hinsche, P. Zahn, I. Mertig, W. Bensch, L. Kienle, *Phys. Status Solidi A* **2016**, *213*, 662.

[10] A.-L. Hansen, T. Dankwart, M. Winkler, J. Ditto, D. C. Johnson, J. D. König, K. Bartholomé, L. Kienle, W. Bensch, *Chem. Mater.* **2014**, *26*, 6518.

[11] M. Winkler, X. Liu, J. D. König, S. Buller, U. Schürmann, L. Kienle, W. Bensch, H. Böttner, *J. Mater. Chem.* **2012**, *22*, 11323.

[12] J. D. König, M. Winkler, S. Buller, W. Bensch, U. Schürmann, L. Kienle, H. Böttner, *J. Electronic Mater*. **2011**, *40*, 1266.

[13] S. Heimann, S. Schulz, J. Schaumann, A. Mudring, J. Stötzel, G. Schierning, *J. Mater. Chem. C* **2015**, *3,* 10375.

[14] S. Schulz, S. Heimann, J. Friedrich, M. Engenhorst, G. Schierning, W. Assenmacher, *Chem. Mater*. **2012**, *24*, 2228.

[15] G. Bendt, S. Schulz, S. Zastrow, K. Nielsch, *Chem. Vap. Deposit.* **2013**, *19*, 235.

[16] S. S. Garje, D. J. Eisler, J. S. Ritch, M. Afzaal, P. O'Brien, T. Chivers, *J. Am. Chem. Soc*. **2006**, *128*, 3120.

[17] G. Gupta, J. Kim, *Dalton Trans*. **2013**, *42*, 8209.

[18] S. L. Benjamin, C. H. de Groot, A. L. Hector, R. Huang, E. Koukharenko, W. Levason, G. Reid, *J. Mater. Chem. C* **2015**, *3*, 423.

[19] R. Huang, S. L. Benjamin, C. Gurnani, Y. Wang, A. L. Hector, W. Levason, G. Reid, C. H. De Groot, *Sci. Rep.* **2016**, *6*, 27593.

[20] S. Schulz, *Coord. Chem. Rev*. **2015**, *297-298*, 49.

[21] G. Bendt, A. Weber, S. Heimann, W. Assenmacher, O. Prymak, S. Schulz, *Dalton Trans.* **2015**, *44*, 14272.

[22] S. L. Benjamin, C. H. de Groot, C. Gurnani, A. L. Hector, R. Huang, W. Levason, G. Reid, *J. Mater. Chem. A* **2014**, *2*, 4865.

[23] H. J. Breunig, H. Jawad, *J. Organomet. Chem.* **1984**, *277*, 257.

[24] A. J. Asche III, E. G. Ludwig, *J. Organomet. Chem.* **1986**, *308*, 289.

[25] S. Heimann, A. Kuczkowski, D. Bläser, C. Wölper, R. Haack, G. Jansen, S. Schulz, *Eur. J. Inorg. Chem.* **2014**, *28*, 4858.

[26] C. D. Wagner, A. V. Naumkin, A. Kraut-Vass, J. W. Allison, C. J. Powell, J. R. Jr. Rumble, NIST Standard Reference Database 20, Version 3.4 (web version) (http:/srdata.nist.gov/xps/) 2003.

[27] H. Bando, K. Koizumi, Y. Oikawa, K. Daikohara, V. A. Kulbachinskii, H. Ozaki, *J. Phys. Condens. Matter* **2000**, *12*, 5607.

[28] C. R. Thomas, M. K. Vallon, M. G. Frith, H. Sezen, S. K. Kushwaha, R. J. Cava, J. Schwartz, S. L. Bernasek, *Chem. Mater*. **2016**, *28*, 35.

[29] E. J. Menke, M. A. Brown, Q. Li, J. C. Hemminger, R. M. Penner, *Langmuir* **2006**, *22*, 10564.

[30] M. Loor, G. Bendt, U. Hagemann, C. Wölper, W. Assenmacher, S. Schulz, *Dalton Trans.* **2016**, *45*, 15326.

[31] C. R. Thomas, M. K. Vallon, M. G. Frith, H. Sezen, S. K. Kushwaha, R. J. Cava, J. Schwartz, S. L. Bernasek, *Chem. Mater*. **2016**, *28*, 35.

[32] T. Sarnet, T. Hatanpa, E. Puukilainen, M. Mattinen, M. Vehkamaki, K. Mizohata, M. Ritala, M. Leskela, *J. Phys. Chem. A* **2015**, *119*, 2298.

[33] S. Zastrow, J. Gooth, T. Boehnert, S. Heiderich, W. Toellner, S. Heimann, S. Schulz, K. Nielsch,

Semicond. Sci. Technol. **2013**, *28*, 035010.

[34] C. Bae, T. Bohnert, J. Gooth, S. Lim, S. Lee, H. Kim, S. Heimann, S. Schulz, H. Shin, K. Nielsch, *Semicond. Sci. Technol*. **2014**, *29*, 064003.

[35] D. Nminibapiel, K. Zhang, M. Tangirala, H. Baumgart, V.S.K. Chakravadhanula, C. Kübel, V. Kochergin, *ECS Solid State Sci. Technol*. **2014**, *3*, P95.

[36] M. Rusek, T. Komossa, G. Bendt, S. Schulz, *J. Cryst. Growth* **2017**, *470*, 128.

[37] P. I. Kuznetsov, V. O. Yapaskurt, B. S. Shchamkhalova, V. D. Shcherbakov, G. G. Yakushcheva,. A. Luzanov, V. A. Jitov, *J. Cryst. Growth* **2016**, *455*, 122.

[38] A. C. Jones, P. O'Brien, *CVD of Compounds Semiconductors: Precursor Synthesis, Development and Applications*, p. 152 ff, VCH, Weinheim, **1997**.

[39] J.-H. Park, T. S. Sudarshan, *Chemical Vapor Deposition*, p. 16 ff, ASM International, **2001**.

[40] a) J. E. Hails, D. J. Cole-Hamilton, W. Bell, *J. Cryst. Growth* **1994**, *145*, 596-601; b) J. E. Hails, D. J. Cole-Hamilton, A. E. D. McQueen, *J. Cryst. Growth* **1998**, *183*, 594-603.

[41] G. Bendt, S. Schulz, unpublished results.

DOI: 10.1016/j.jcrysgro.2018.03.021
URN: urn:nbn:de:hbz:464-20201215-150815-8

This is the Authors Accepted Manuscript of an article published in: Journal of Crystal Growth 2018, Volume 490, Pages 77-83.
The final version may be found at: https://doi.org/10.1016/j.jcrysgro.2018.03.021